

The measurement of gain on the 1.315 μm transition of atomic iodine in a subsonic flow of chemically generated $\text{NCl}(a^1\Delta)$

John M. Herbelin, Thomas L. Henshaw^{*}, Brent D. Rafferty, Brian T. Anderson, Ralph F. Tate, Timothy J. Madden, Gerald C. Manke II, Gordon D. Hager

Air Force Research Laboratory, Kirtland AFB, 3550 Aberdeen Avenue SE, Kirtland AFB, NM 87117-5776, USA

Received 25 September 1998; in final form 10 November 1998

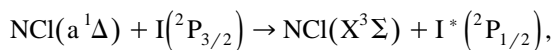
Abstract

Gain is measured on the electronic $\text{I}(^2\text{P}_{3/2})\text{--I}^*(^2\text{P}_{1/2})$ transition of atomic iodine at 1.315 μm when hydrazoic acid HN_3 is injected into a flow of iodine and chlorine atoms. The inversion was generated in a transverse subsonic flow device that produced electronically excited $\text{I}^*(^2\text{P}_{1/2})$ atoms from the efficient energy transfer reaction between $\text{NCl}(a^1\Delta)$ metastable and ground state $\text{I}(^2\text{P}_{3/2})$ atoms. The population inversion was directly observed using a 1.315 μm tunable diode laser that scanned the entire line shape of the (3,4) hyperfine transition of iodine. © 1999 Elsevier Science B.V. All rights reserved.

1. Introduction

Metastable atoms and diatomic molecules have long been recognized for their importance as energy carriers in laser media. For example, in the near-infrared COIL chemical laser system [1,2] the $\text{O}_2(a^1\Delta)$ metastable pumps the $\text{I}^*(^2\text{P}_{1/2}) \rightarrow \text{I}(^2\text{P}_{3/2})$ lasing transition at 1.315 μm through the resonant energy transfer reaction between $\text{O}_2(a^1\Delta)$ and ground state $\text{I}(^2\text{P}_{3/2})$. Similarly, chemically generated nitrene metastables such as $\text{NCl}(a^1\Delta)$ and $\text{NF}(a^1\Delta)$ have been under investigation for a number of years as an energy source to power an electronic transition chemical laser [3–5]. Following the discovery of the

efficient transfer of electronic energy between $\text{NCl}(a^1\Delta)$ and atomic iodine,



$$k_{300} = 2 \times 10^{-11} \text{ cm}^3/\text{s} \quad (1)$$

increased attention has been directed toward the demonstration of gain and or lasing on the 1.315 μm transition of the atomic iodine excited by $\text{NCl}(a^1\Delta)$. In 1992, evidence of a population inversion in a subsonic flow using ICl as a source of iodine [8] was presented and shortly thereafter near threshold laser oscillation was observed from the photolysis (193 nm) of mixtures containing ClN_3 and CH_2I_2 [9]. Unfortunately, due to the near threshold conditions involved in both of these experiments, the results could not be quantified and it was felt that a direct measurement of gain would be the logical next step in the investigation of this system. In this regard, we

^{*} Corresponding author. Fax: +1 505 846 4807; E-mail: henshawt@plk.af.mil

present a sensitive and direct measurement of the population inversion between the $I(^2P_{3/2})$ and $I^*(^2P_{1/2})$ states of atomic iodine produced by energy transfer from $\text{NCl}(a^1\Delta)$.

2. Experimental

The gain determination reported here was made in a transverse subsonic flow reactor equipped with sensitive optical diagnostics for measuring chemiluminescent emissions and ground state iodine atom absorption. The approach in this study follows the general methodology used by earlier investigators [6,8,10] with a few notable exceptions. By far the most important is the use of a tunable diode laser probe system. The device is a continuously tunable single-mode 1.315 μm laser (New Focus model 6248) that provides single line lasing with a spectral line width (FWHM) of < 500 kHz over 30 GHz from 7602.4 to 7603.5 cm^{-1} . With this apparatus it was possible to scan across the $I(^2P_{3/2})$ – $I^*(^2P_{1/2})$ transition with complete hyperfine resolution and obtain excellent signal to noise ratios at extremely small signal levels [11]. The experimental layout for the system diagnostics is presented in Fig. 1 and includes an Optical Multi-channel Analyzer, OMA,

(PAR, model 1412) mounted on a 1/4 m monochromator (Jarrell–Ash), a 1/3 m McPherson Spectrometer equipped with an intrinsic Ge detector (ADC, model 403L) and the diode laser. Near-infrared emissions, $\text{NCl}(a^1\Delta\text{--}X^3\Sigma)$ at 1.08 μm , $\text{NF}(a^1\Delta\text{--}X^3\Sigma)$ at 0.874 μm and $I(^2P_{1/2}\text{--}^2P_{3/2})$ at 1.315 μm , were measured via the 1/3 m McPherson-Ge detector system. Emission stemming from the $\text{NCl}(b^1\Sigma\text{--}X^3\Sigma)$ transition was dispersed and detected with the 1/4 m monochromator/OMA arrangement. All emissions were absolutely calibrated using a black body source.

The transverse flow facility, shown schematically in Fig. 2, was designed to allow sequenced injection of the reactants. Molecular fluorine F_2 (20% in He) was passed through a D.C discharge under conditions that dissociated $> 95\%$ of the F_2 . The conversion efficiency was determined previously by a titration technique using excess hydrogen iodide [12]. Near unit conversion was required in order to avoid formation of IF, an effective quencher of $I^*(^2P_{1/2})$, that was observed when F_2 was present in the flow stream. It is important to note that at F_2 flow rates above 1.0 mmol/s a significant decline in the degree of F_2 dissociation occurs thus limiting our F density to conditions described here.

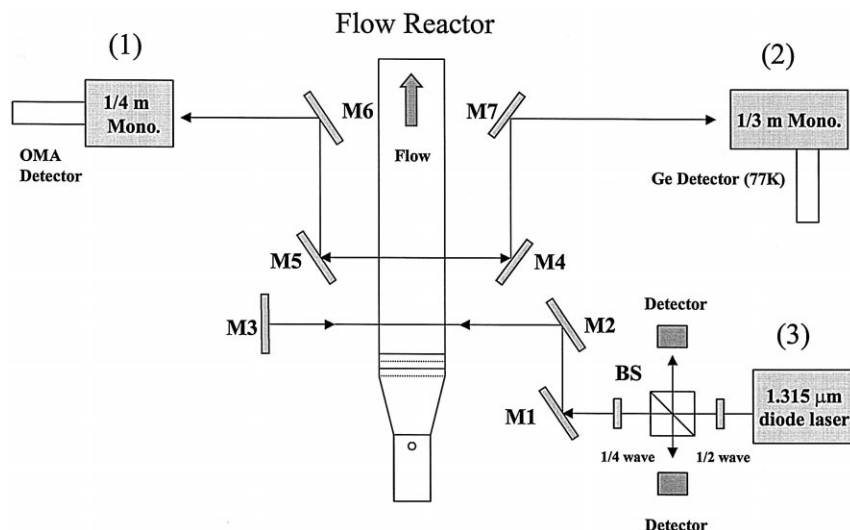


Fig. 1. Layout of the optical diagnostics including an (1) Optical Multi-channel Analyzer, OMA, on a 1/4 m Jarrell-Ash Spectrometer, (2) Intrinsic Ge detector mounted on a 1/3 m McPherson spectrometer and (3) the scanning diode laser with appropriate monitoring apparatus. M1–M7, mirrors; BS, beam splitter.

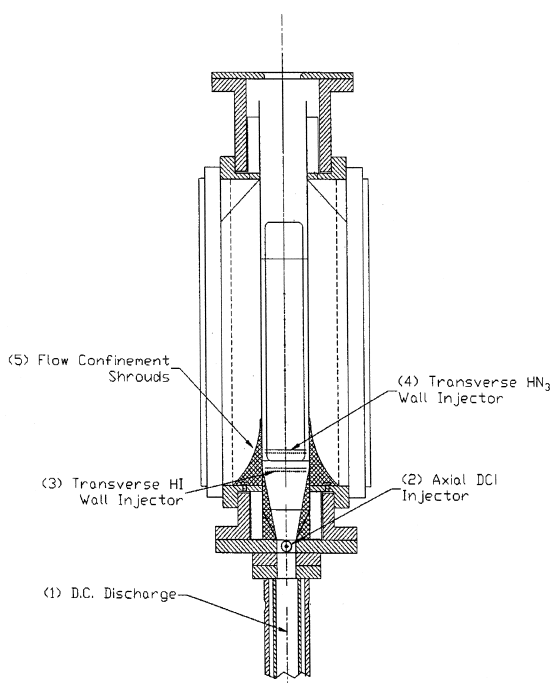
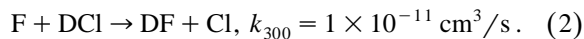
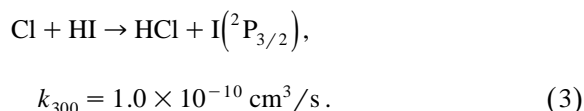


Fig. 2. Schematic representation of the flow device showing (1) dc discharge, (2) axial injector (DCI), (3) first set of transverse wall injectors (HI), (4) second set of transverse wall injectors (HN_3) and (5) flow confinement shrouds.

Upon exiting the discharge region, excess deuterium chloride, DCI, was injected along with helium via an axial injector to produce the desired Cl atoms [13]:



A sufficient distance of about 10 cm, which translates to approximately 0.26 ms, was provided to allow this reaction to run to completion. Through the first set of transverse wall injectors we introduced hydrogen iodide, HI, along with a carrier flow of helium to ensure proper penetration. This produced a flow of ground state iodine atoms via the reaction [14],



The presence of ground state iodine atoms was readily monitored with the diode laser probe. A typical absorption spectrum of the (3,4) transition is shown by the negative curve in Fig. 3.

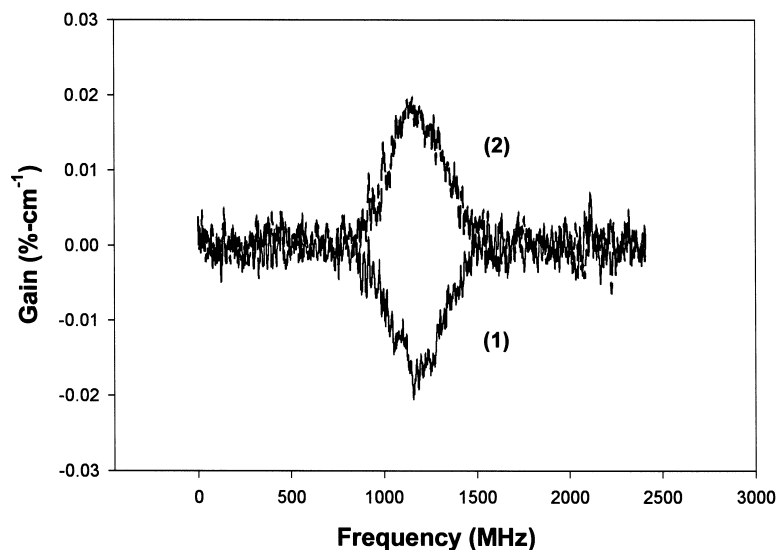
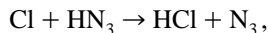
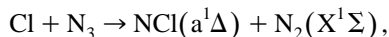


Fig. 3. The observed (1) absorption and (2) gain line shape profiles for the (3,4) transition of the $\text{I}({}^2\text{P}_{1/2} \rightarrow {}^2\text{P}_{3/2})$ transition at $1.315 \mu\text{m}$. Flow conditions for (1) absorption: 16 Torr total pressure, 0.7 mmol/s F_2 , 2.0 mmol/s DCI, 0.03 mmol/s HI, 0 mmol/s HN_3 ; (2) gain: 16 Torr total pressure, 0.7 mmol/s F_2 , 2.0 mmol/s DCI, 0.03 mmol/s HI, 3.3 mmol/s HN_3 . Note that the frequency axis is expressed as a relative frequency obtained by mapping the absorption spectrum to the 300 MHz spacing of the transmission peaks of the Fabry–Perot interferometer.

When a diluted mixture of HN_3 was introduced via the second set of transverse wall injectors, $\text{NCl}(a^1\Delta)$ was produced according to the reaction,



$$k_{300} = 1 \times 10^{-12} \text{ cm}^3/\text{s} \quad (4a)$$



$$k_{300} = 2 \times 10^{-11} \text{ cm}^3/\text{s} \quad (4b)$$

which is believed to be around 75% efficient (Eq. (4a) [15]; Eq. (4b) [16]). The reported rate coefficients here are for room temperature and as such, it is unlikely that sufficient $\text{NCl}(a^1\Delta)$ would be generated from the $\text{Cl} + \text{HN}_3$ reaction. However, measured reactor flow temperatures under these conditions approach 475 K and a significant enhancement in the magnitude of this rate constant is expected. Indeed, preliminary data from temperature dependent rate measurements of reaction 4a and model calculations suggest a 6–7-fold increase in the rate coefficient is observed at this temperature [17].

Hydrogen azide, HN_3 , was synthesized by the reaction of molten stearic acid ($\text{CH}_3(\text{CH}_2)_{16}\text{COOH}$) with sodium azide (NaN_3) under vacuum at 110°C. A 10:1 molar excess of stearic acid over sodium azide was used. The gaseous HN_3 was stored as a 5% or 10% mixture in helium. Helium diluent (Matheson, 99.995%), F_2 (Matheson, 20% in helium), DCl (Cambridge Isotopes, 99%), HI (Matheson, 99%) were used without further purification.

3. Results and discussion

Under the flow conditions provided in Table 1, the previous absorption curve was reversed to the

positive direction as shown in Fig. 3. The magnitude of the peak gain, 0.02%/cm, provides an estimate of the fraction of the ground state iodine atoms converted to the excited $\text{I}^*(^2\text{P}_{1/2})$ state. Accordingly, using the following equation for gain,

$$g = \sigma \left\{ \left[\text{I}^*(^2\text{P}_{1/2}) \right] - 1/2 \left[\text{I}(^2\text{P}_{3/2}) \right] \right\} \quad (5)$$

where σ is the temperature corrected cross-section for stimulated emission, $1.3 \times 10^{-16}/\sqrt{T}$ in cm^2 , and noting that the total iodine concentration in the system is constant,

$$[\text{I}]_T = \left[\text{I}^*(^2\text{P}_{1/2}) \right] + \left[\text{I}(^2\text{P}_{3/2}) \right] \quad (6)$$

quantitative equations relating the $\left[\text{I}^*(^2\text{P}_{1/2}) \right]$ and $\left[\text{I}(^2\text{P}_{3/2}) \right]$ density under gain conditions can be generated [18]. Solving Eqs. (5) and (6) for $\left[\text{I}^*(^2\text{P}_{1/2}) \right]$ and $\left[\text{I}(^2\text{P}_{3/2}) \right]$ yields

$$\left[\text{I}(^2\text{P}_{3/2}) \right] = 2/3[\text{I}]_T - 2/3(g/\sigma) \quad (7)$$

$$\left[\text{I}^*(^2\text{P}_{1/2}) \right] = 1/3[\text{I}]_T + 2/3(g/\sigma). \quad (8)$$

For an $[\text{I}]_T = 6.0 \times 10^{13} \text{ cm}^{-3}$, measured prior to introducing HN_3 to the flow system, and the peak gain from Fig. 3, the $[\text{I}^*]$ and $[\text{I}]$ densities are 4.0×10^{13} and $2.0 \times 10^{13} \text{ cm}^{-3}$, respectively. Thus 2/3 of the available ground state iodine atoms are converted to the $\text{I}^*(^2\text{P}_{1/2})$ state, a result that confirms previous measurements that the $\text{NCl}(a^1\Delta) + \text{I}(^2\text{P}_{3/2})$ reaction system is an efficient process for generating $\text{I}^*(^2\text{P}_{1/2})$ [6,7,16].

The maximum small signal gain (g_{max}) is obtained when all the iodine is converted to the $^2\text{P}_{1/2}$ state. Under these conditions Eq. (5) reduces to $g_{\text{max}} = \sigma[\text{I}]_T$ and the maximum gain expected is 0.036%/cm. However, scaling the system to higher flow rates failed to generate total inversion of ground

Table 1

Typical flow reactor conditions for the observed population inversion stemming from the $\text{I}(^2\text{P}_{3/2}) - \text{I}^*(^2\text{P}_{1/2})$ transition

Reagent species	Molar rate (mmol/s)	Flow	Reactor pressure (Torr)	Reagent density (cm^{-3})	Cross-sectional area (cm^2)	Flow velocity (cm/s)	Flow temperature (K)
He	151.28		15.50	3.0×10^{17}	10	3.0×10^4	470
F_2	0.66			1.3×10^{15}			
DCl	2.00			4.0×10^{15}			
HN_3	3.32			6.6×10^{15}			
HI	0.032			6.3×10^{13}			
Total	157.29			3.1×10^{17}			

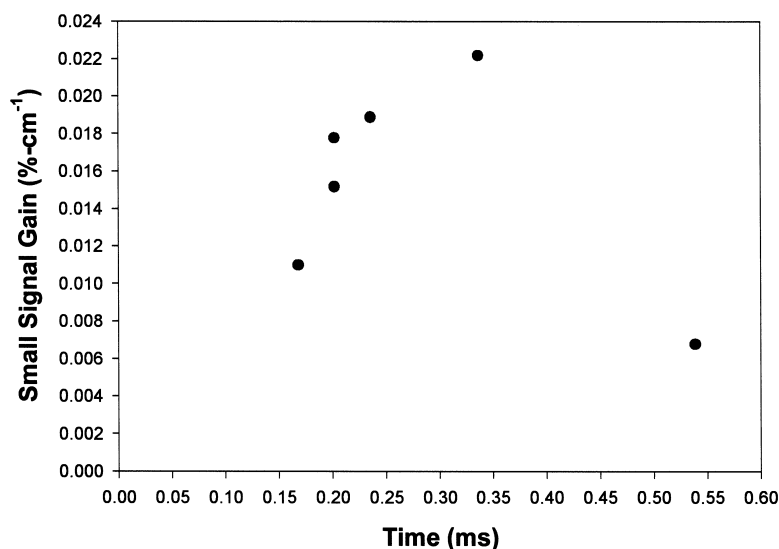
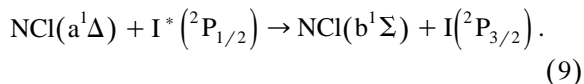


Fig. 4. The $I(^2P_{3/2}) - I^*(^2P_{1/2})$ gain zone resulting from the $NCl(a^1\Delta) + I(^2P_{3/2}) \rightarrow I^*(^2P_{1/2}) + NCl(X^3\Sigma)$ reaction. The gain profile extends over a reasonably long flow time of nearly 0.5 ms.

state iodine atoms. It is not known at this time if the system is limited by the $I^*(^2P_{1/2})$ branching fraction or other loss mechanisms. One system limitation is traceable to the dc discharge efficiency and its failure to generate large F atom densities without incurring significant $I^*(^2P_{1/2})$ and/or $NCl(a^1\Delta)$ removal. Fig. 4 presents a zone profile of gain under similar conditions described in Table 1. The gain was found to extend well over the field of view from the terminus of the flow confinement shroud at 0.17 ms (5 cm) to beyond 0.53 ms (16 cm) where the flow begins to break up in this device or possible collisional deactivation of the energy carriers occur. This long zone length is not surprising since the flow conditions were chosen to minimize deactivation. These observations were very reproducible over a range of conditions.

Under these same flow conditions, the emission from the excited $NCl(b^1\Sigma)$ state was enhanced, just as observed by earlier investigators [19]. This indicated that the primary source of the $NCl(b^1\Sigma)$ was via the energy transfer process,



The $NCl(b^1\Sigma^+ - X^3\Sigma^-)$ emission at 665 nm was readily observed visually as well as with the OMA

and acted as a most convenient indicator of when the flows were properly optimized for maximum gain. If the DCI flow was turned off, then the visual emission would change from bright red–orange to bright green corresponding to 530 nm, $NF(b^1\Sigma^+ - X^3\Sigma^-)$ emissions in the reaction zone. This emission was also monitored utilizing the Optical Multi-channel Analyzer, OMA, and served as an excellent method for determining when sufficient DCI had been added to assure complete conversion of the F atoms to Cl atoms.

4. Conclusions

A direct measurement of the population inversion between the $I(^2P_{3/2}) - I^*(^2P_{1/2})$ states of iodine resulting from the $NCl(a^1\Delta) + I(^2P_{3/2})$ reaction has been observed. This represents a significant step in the development of an all gas phase iodine laser. The observed gains were substantially lower (approximately a factor of 50) than that of the familiar chemical oxygen iodine laser (COIL). To obtain a meaningful laser demonstration a significant enhancement in the small signal gain is essential. The current experimental result is limited by number

density, specifically the F atom concentration. Accordingly, future experiments will be directed at increasing the F atom number density and determining whether or not the $\text{NCl}(a^1\Delta)/\text{I}^*(^2\text{P}_{1/2})$ system will scale to appropriate levels for a successful laser demonstration. If these scaling experiments are achieved then the practical demonstration of a nitrene based cw iodine laser is imminent.

References

- [1] W.E. McDermott, N.R. Pchelkin, D.J. Benard, R.R. Bousek, *Appl. Phys. Lett.* 32 (1978) 469.
- [2] D.J. Benard, W.E. McDermott, N.R. Pchelkin, R.R. Bousek, *Appl. Phys. Lett.* 34 (1979) 40.
- [3] J.M. Herbelin, N. Cohen, *Chem. Phys. Lett.* 20 (1973) 605.
- [4] A.T. Pritt Jr., R.D. Coombe, *Int. J. Chem. Kinet.* 12 (1980) 741.
- [5] X. Liu, M.A. MacDonald, R.D. Coombe, *J. Phys. Chem.* 96 (1992) 4907, and references therein.
- [6] R.D. Bower, T.T. Yang, *J. Opt. Soc. Am. B.* 8 (1991) 1583.
- [7] A.J. Ray, R.D. Coombe, *J. Phys. Chem.* 97 (1993) 3475.
- [8] T. Yang, V.T. Gylys, R.D. Bower, L.F. Rubin, *Opt. Lett.* 24 (1992) 1803.
- [9] A.J. Ray, R.D. Coombe, *J. Phys. Chem.* 99 (1995) 7849.
- [10] A.T. Pritt Jr., D. Patel, R.D. Coombe, *Int. J. Chem. Kinet.* 16 (1984) 977, see for example.
- [11] R.F. Tate, B.T. Anderson, P.B. Keating, G.D. Hager, *Proc. SPIE, Gas Chem. Lasers Intense Beam Appl.* 3268 (1998) 115.
- [12] B.D. Rafferty, B.T. Anderson, T.L. Henshaw, J.M. Herbelin, G.D. Hager, *Lasers* 97 (1997) 23.
- [13] M.A.A. Clyne, W.S. Nip, *Int. J. Chem. Kinet.* 10 (1978) 367.
- [14] F.J. Wodarczyk, C.B. More, *Chem. Phys. Lett.* 26 (1974) 484.
- [15] G.C. Manke II, D.W. Setser, *J. Phys. Chem.* 102 (1998) 153.
- [16] T.L. Henshaw, S.D. Herrera, L.A. Schlie, *J. Phys. Chem.* 102 (1998) 6239.
- [17] G.C. Manke II, T.J. Madden, unpublished results, 1998.
- [18] G.D. Hager, C.A. Helms, K.A. Truesdell, D. Plummer, J. Erkkila, P. Crowell, *IEEE J. Quantum Electron.* 32 (1996) 1525.
- [19] T.T. Yang, *Proc. SPIE, Intense Beams Appl.: Laser, Ions, Microwaves* 2119 (1997) 122.